Estimation of extreme daily precipitation thermodynamic scaling using gridded satellite precipitation products over tropical land

Rémy Roca

Estimation of extreme daily precipitation thermodynamic scaling using gridded satellite precipitation products over tropical land

Environmental Research Letters

LETTER

Estimation of extreme daily precipitation thermodynamic scaling using gridded satellite precipitation products over tropical land

Rémy Roca
Observatoire Midi-Pyrénées, LEGOS, Toulouse, France
E-mail: remy.roca@legos.obs-mip.fr

Keywords: extreme precipitation, tropics, satellite observations
Supplementary material for this article is available online

OPEN ACCESS

RECEIVED
25 March 2019

REVISED
24 July 2019

ACCEPTED FOR PUBLICATION
25 July 2019

PUBLISHED
18 September 2019

Abstract

This study explores the tropical land distribution of precipitation and its extremes focusing on the daily $1^\circ \times 1^\circ$ scale. A common period of 5-year over the tropical belt (30°s–30°n) corresponding to more than 39 million data points, is used to highlight the robust (and non-robust) observed features. A set of 10 observational products is analyzed ranging from satellite only to rain gauges only products and various blended intermediates as well as a sub ensemble of satellite-based products relying upon microwave observations. Overall, the various datasets show a small diversity of response as far as tropical land mean precipitation is concerned. When sorted by surface temperature, the spread in mean rainfall is also well below 10% over a large span of the surface temperature regime. The consistency between the surface temperature and the extreme precipitation is further investigated by computing the thermodynamic scaling of daily precipitation extreme with surface temperature. The wet days' 99.9th and 99th percentiles are considered and corresponds to 'extreme' extremes (~110 mm d^{-1}) and 'moderate' extremes (~60 mm d^{-1}), respectively. The analysis reveals three regimes over the 287–305 K 2 m temperature range. In the cold regime, 287–293 K, extremes exhibit no dependence to surface temperature while in the warm regime, 299–305 K, the extremes decrease with temperature as identified in previous studies. Over the 293–299 K regime, the scaling of the sub ensemble of satellite products is ~5.2 K/% for the 'extremes' extremes and 5.0% for the 'moderate' extremes, and is robust throughout the sub ensemble. This analysis fills the regional gap of previous conventional data based studies and further confirms the Clausius–Clapeyron theoretical expectation for the tropical land regions.

1. Introduction

Global energy budget considerations provide a strong constraint of global precipitation owing to the coupling between energy and water budgets and offer a physically sound theoretical pathway to explore the future evolution of precipitation under climate warming through changes of the atmospheric water vapor content (Ramanathan 1981). Thermodynamics indeed dictates an increase of the atmospheric water vapor content under warming at a rate of 6%–7%/K which translates in a 2%–3%/K increase in global mean precipitation via the induced radiative cooling closure enforcement of the water and energy budget (Stephens and Ellis 2008). This thermodynamically constrained alteration of the atmospheric water vapor also has consequence on local precipitation events and a moister atmosphere is expected to yield stronger local precipitation (Trenberth 2011 and reference therein). The scaling of the high rainfall percentiles to surface temperature as depicted by the conventional observations (rain gauges), have been extensively used to explore the recent evolution of the precipitation extremes over land and its associated scaling with temperature (e.g. Westra *et al* 2013). Extreme precipitation from the gauges have further been shown to well agree with theoretical expectations and climate models results at least in the mid-latitudes (Fischer and Knutti 2016). Indeed, these observations are by essence mainly concentrated over data rich areas of the

globe, leaving an unsatisfactory appraisal of the evolution of intense rainfall over conventional data poor regions like the tropical land regions (Becker *et al* 2013, Kidd *et al* 2017, Taylor *et al* 2017). The lack of data yields to a series of non-robust results about the scaling of daily extreme precipitation to temperature in the tropics (Utsumi *et al* 2011, Eiji *et al* 2012, Vittal *et al* 2016, Bao *et al* 2017, Barbero *et al* 2017, Wang *et al* 2017, Ali and Fowler 2018). A large number of multi-source gridded precipitation products, including multiple satellites observations and microwave constellation-based products, has emerged in the recent decade (Levizzani *et al* 2018) that could help to alleviate this regional gap and clarify the observational relationship between precipitation extremes and surface temperature in the tropics. At daily scale satellite gridded products indeed exhibit significant skills at documenting meteorological variability in the tropics (Roca *et al* 2010, Gosset *et al* 2013, Guilloteau *et al* 2016), if not for the documentation of the extremes, and are characterized by improvements of the recent generation of products over the previous ones (Maggioni *et al* 2016, Beck *et al* 2017). Despite the importance of the local scaling at daily scale, studies addressing tropical land-wide statistics using gridded data based are not numerous with the exception of (Wasko *et al* 2016) for which a single gridded product is used that suggests the satellite observations are offering an alternative to stations based estimates.

The scaling of extreme precipitation to surface temperature can be derived from physical considerations. Precipitation at the surface results from the condensation of water vapor in the atmosphere and subsequent fall out to the ground. The net condensation rate of the atmosphere is indeed the outcome of the complex interplay between the thermodynamic profiles of the column, the intensity of convection, the cloud and rain microphysics and in particular to the tropics, the mesoscale dynamics of the cloud system (e.g. Roca *et al* 2017). Despites this complexity, in the tropics, following atmosphere dry static energy budget considerations and focusing on extreme conditions, extreme precipitation rate (P_e) can be expressed (O'Gorman and Schneider 2009) as

$$P_e = -\epsilon \left\{ \omega_e \frac{dq_s}{dp} \bigg|_{\theta*} \right\}, \quad (1)$$

where ω_ε is the vertical velocity in pressure coordinates, q_s the specific humidity at saturation at constant equivalent potential temperature (θ^*) and ε is the measure of the precipitation efficiency related to the microphysics of the rain and the {.} sign indicates the vertical averaging operator. At daily scales, the sensitivity of P_e to efficiency can be neglected (Singh and O'Gorman 2014) and the physical scaling (1) further simplifies to a dynamical and a thermodynamical contributions. For tropical conditions, idealized cloud resolving model simulations suggest a weak dynamical response to large perturbations of surface temperature (Muller *et al* 2011, O'Gorman 2015 its figure 3; Pfahl *et al* 2017). Considering weak variations in the vertical velocity and further assuming a simple tropical divergence profile, the fractional change in P_e scales with fractional change of saturation humidity at the surface (O'Gorman and Schneider 2009) and further reads

$$\frac{\delta P_e}{P_e} \propto \frac{\delta q_s^{surface}}{q_s^{surface}}. \quad (2)$$

The near surface air saturation humidity is a function of temperature alone and pressure and equation (2) simply states that the fractional change of extreme precipitation scales with near surface air temperature at the rate of change of the Clausius–Clapeyron law with near surface air temperature. Under typical tropical conditions, this thermodynamic scaling is close to 6%–7%/K (Trenberth *et al* 2003). Therefore, near surface temperature is used to assess the scaling within the gridded precipitation products. By essence, the physical scaling hence is valid under assumptions that restrict its use to the regime for which surface humidity increases with surface temperature. Indeed, at the warm end of the range of surface air temperature (like Sahara) rain rarely occurs. Hence, it should be considered that the near air temperature is only a proxy for near surface air humidity at saturation and the range of meaning of the physical scaling is further discussed below. The estimation of the physical scaling does not need to reflect the time evolution of the extreme precipitation under recent climate change. The physical scaling is a way to 'map' the precipitation distribution over regimes of surface air temperature (rather than geographical locations) that further links the precipitation to its local environment. Such physical scaling is not to be misinterpreted or compared with other proposed scaling in the literature based on co-variability of precipitation extremes with various surface temperature indicators ranging from globally averaged surface temperature, global ocean surface mean temperature or regional composite of temperature (Westra and Sisson 2011, Liu *et al* 2012). The estimated thermodynamic scaling of precipitation extreme with surface temperature for the current climate should nevertheless be used with caution to discuss the evolution of extreme events with future climate change. Indeed, unaccounted for changes in precipitation frequency (Schär *et al* 2016) or the limited scope of the underlying physical framework to characterize the future evolution of precipitation extremes (Pfahl *et al* 2017) prevents a straight forward interpretation of the scaling. When carefully interpreted the scaling has nevertheless proven itself as a useful metric to narrow the spread in climate models responses (O'Gorman 2012, Bao *et al* 2017), to relate past observed variations of precipitation to surface conditions (Westra *et al* 2014) or to serve as an emerging constraint to climate model ensembles (Allan and

Table 1. Conditional mean precipitation (>1 mm d^{-1}) for the 2012–2016 period over tropical land. Mean, standard deviation and coefficient of variation (or normalized standard devitation) are also reported for the ensemble of all the products and for the sub-set of the ensemble defined in the text.

Name	Conditional mean (mm d^{-1})
TAPR	10.0
TMPA	9.8
GSMArtg	9.3
CMORg	9.5
MSWE	9.7
GPCPun	10.9
PERS	8.2
CHIRg	9.2
GPCC	11.9
GPCCfg	9.1
Ens Mean	9.8
Ens std	1.0
Ens cvar (%)	10.6
sEns Mean	9.7
sEns std	0.3
sEns cvar (%)	2.7

Liu 2018). At daily scales, the scaling of high percentile with surface temperature has been vastly used in various previous studies (O'Gorman 2015 and references therein).

The main objective of this paper is hence to fill the regional gap over the tropical land using a large set (and a sub set) of gridded products and to investigate the robust and non-robust features among the products for various metrics of the tropical precipitation distribution and its extremes. A secondary aim of this paper is to explore the ability of the gridded products to provide a robust (or not) perspective on the thermodynamic scaling of precipitation extremes to the surface temperature over the tropical land in the current climate.

To simplify the reading of the letter, the description of the full products ensemble and the rationale for selecting a subset ensemble are discussed in the supplementary material data section. Similarly, the methodological aspects of the scaling computation are detailed in the Supplementary Material Methods section. The analysis of the full distribution of daily-accumulated precipitation is presented next. Section 3 is devoted to the results of the scaling and the papers ends with a conclusion/discussion section.

2. The tropical land precipitation distribution

2.1. The tropical precipitation distribution over land

Mean conditional precipitation, i.e. mean precipitation when precipitation is greater than 1 mm d^{-1}, over tropical land is remarkably consistent among the various products (table 1) with a mean value of 9.8 mm d^{-1} +- 10% for the entire ensemble. The sub-ensemble products exhibit the same average value with even less spread among the products (3%). The occurrence of daily accumulated precipitation at 1° × 1° over tropical land for the 2012–2016 period spans 5–6 order of magnitude over the 0–275 mm d^{-1} range for each product (figure 1 top). All the products share a similar shape for the distribution. Above 25 mm d^{-1}, the GPCC product occurrence is systematically higher than all the other products while the PERSIANN record shows the lowest occurrence systematically.

While the mean value is very robust among the products, the distribution is not. We note that here the distribution is explored up to 275 mm d^{-1} which correspond to very heavy rain accumulation. The relationship between the tropical wide rainfall accumulation and the percentiles of the distribution is presented in figure S1 is available online at stacks.iop.org/ERL/14/095009/mmedia.

The spread among the whole ensemble of products increases with the daily accumulated precipitation amount (figure 1 bottom) from 10%–25% up to 50 mm d^{-1} (~99th percentile), and asymptotes around 100% from 100 mm d^{-1} (~99.9th) and above. The spread is considerably less when the sub-ensemble of satellite-based products that includes microwave observations is concerned. Up to 75 mm d^{-1}, the spread is below 10%. Above 75 mm d^{-1}, the normalized standard deviation increases log-linearly with the daily-accumulated precipitation at 25% for 150 mm d^{-1} (~99.99th) and up to 50% at 200 mm d^{-1} (~99.999th) and just below 100% at the end of the distribution.

2.2. The tropical precipitation distribution sorted by surface temperature over land

When daily-accumulated precipitation is sorted with respect to 2 m temperature regimes, the contribution to the total precipitation peaks around 298 K at a value of ~18% for all of the products (figure 2 top). The distribution from the coldest and the warmest regimes are very similar across the products. The spread among the various products is very small (figure 2 bottom), less than 10% up to 303 K and there is hardly any difference between the ensemble mean distribution and the one from the sub ensemble. This very robust feature of the gridded products can also be interpreted in terms of the various products having a similar geographical distribution of the precipitation. This is expected to some extent, at least for the sub-ensemble, since the products share some of the raw satellite observations. Compared to the ensemble members, the CHIRPS product appears to overestimate slightly the contribution to total rainfall up to 297 K where it peaks and then shows underestimations in the warmer regime. The TAPEER dataset reveals a distribution close to the ensemble mean but with a slightly underestimated maximum contribution at 299 K.

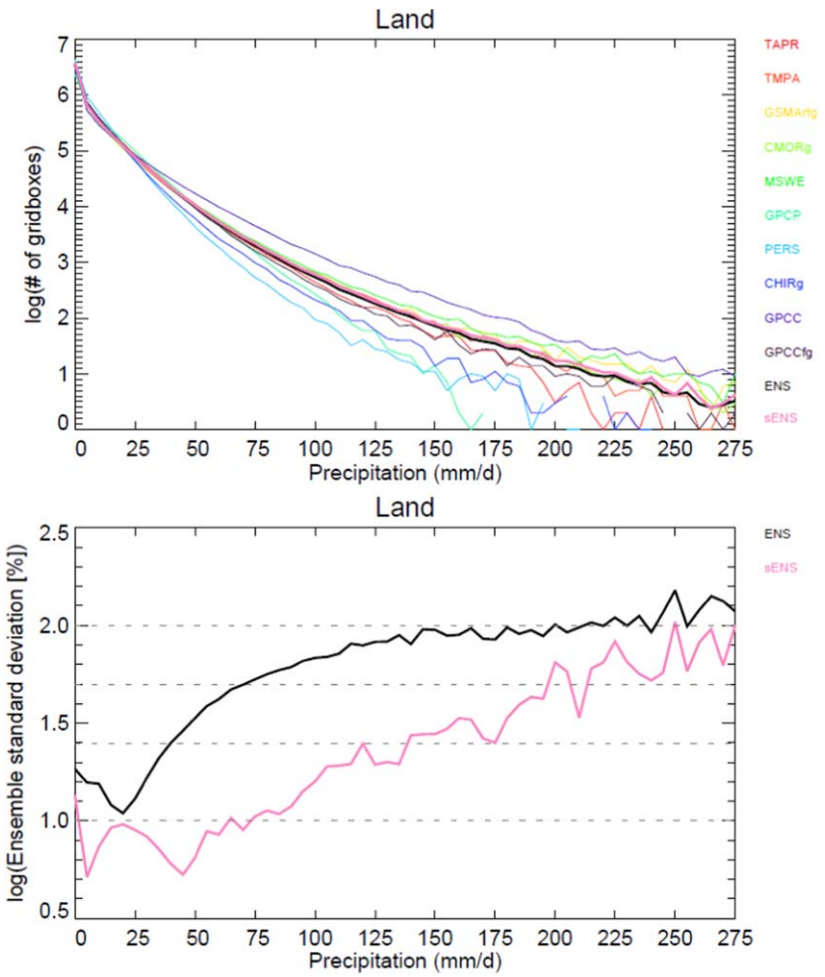

Figure 1. (Top) Distribution of occurrence of daily 1° × 1° accumulated precipitation over the tropical (30°s–30°n) land for the period 2012–2016. The colors correspond to various precipitation datasets listed on the right. (Bottom) the normalized standard deviation of the above distribution across the ensemble of all the products (ENS) and for the sub-set of the ensemble defined in the text (sENS). In the bottom figure, the horizontal dashed gray lines corresponds to the 10%, 25%, 50% and 100% level.

3. The scaling of the extreme of tropical precipitation with surface temperature

The extremes are characterized via the upper wet day percentiles of the distribution for various surface temperature bins (see Supplementary materials: method section). 'Extreme' extremes and the 'moderate' extremes are defined by the 99.9th and the 99th percentile, respectively. The magnitude of these percentiles are ~110 and ~60 mm d^{-1} (figure 3). The use of other metrics or indices to qualify the extremes can limit the considered magnitude of the range of precipitation. For instance, the quasi-global analysis of (Herold *et al* 2017) relies upon the Rx1day index to characterize the 'extreme' extremes which ranges, at the 1° × 1° daily scale, between 35 and 50 mm d^{-1} depending upon the product, much less than the magnitude considered here. Note that statistics for the 90th percentiles are also reported although the intensity under considerations (~25 mm d^{-1}) is generally not associated with the notion of an extremely intense rain event.

The relationship between the extremes of precipitation and the surface temperature for all of the individual products, the entire and the sub ensemble are presented in figures S2, S3 and S4 for the 99.9th, the 99th and the 90th percentiles, respectively. Figure 3 summarizes the results for the 99.9th and the 99th percentiles for the mean of the sub ensemble of products. A spread around 20% for 99.9th and 99th percentiles, and around 15% for the 90th percentile characterize the distribution of the extremes. When the sub ensemble is considered, the spread is reduced significantly around 5% or less over a large part of the temperature range under considerations. For the three percentiles values and for most of the products, the extreme exhibits a 'peak' structure in agreement with previous findings based on rain gauges' data (Hardwick Jones *et al* 2010), reanalysis or climate models (Wang *et al* 2017). The peak is observed around 299–300 K. For most of the products, the 90th percentiles distribution (figure S4) shows two regimes with temperature, increasing up to the peak and decreasing for higher temperature; a feature already identified in various previous studies. On the other hand, for the

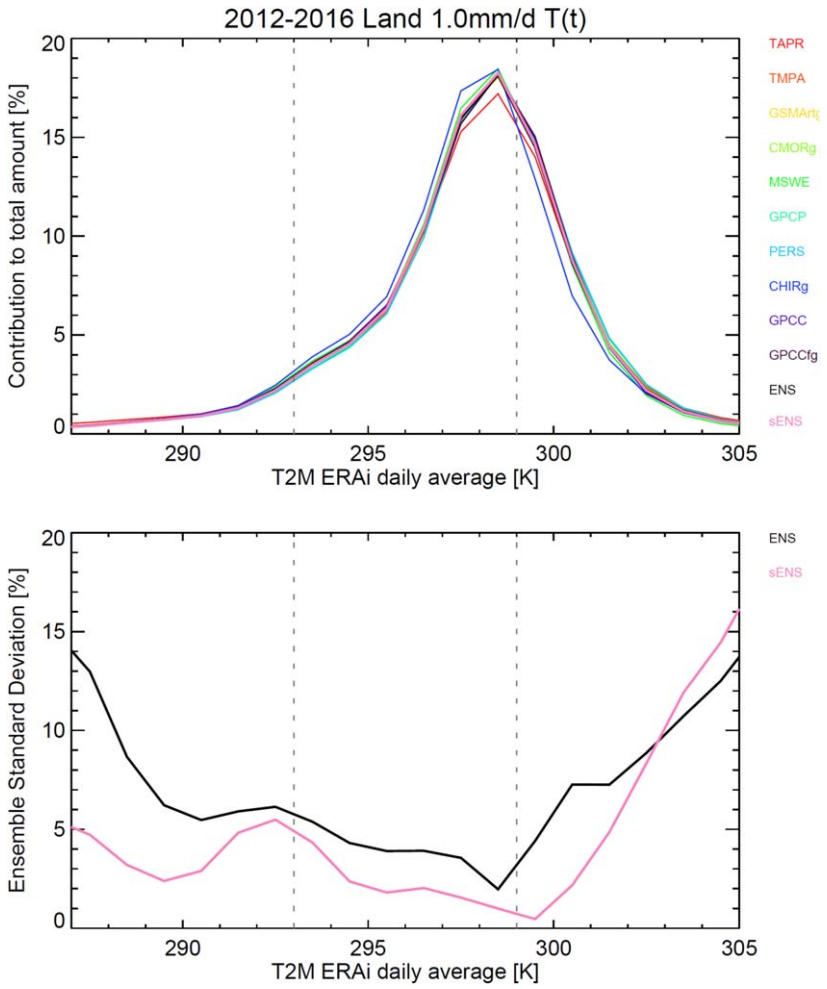

Figure 2. (Top) Contribution (in %) to the total accumulated precipitation over the tropical (30°s–30°n) land for the period 2012–2016 as a function of the 2 m daily temperature. The colors correspond to various precipitation datasets listed on the right. (Bottom) the normalized standard deviation of the above distribution across the ensemble of all the products (ENS) and for the subset of the ensemble defined in the text (sENS).

99.9th and the 99th percentiles, three temperature regimes can be distinguished for most of the products and for the product ensemble and sub ensemble means that differs from point gauges analysis (Westra *et al* 2014) and are detailed next.

3.1. The 'cold' regime (287 K<t2m<293 K)

This regime corresponds to ~6% of the total precipitation (figure 2). In this regime, the extreme precipitation (both at the 99.9th and 99th percentiles) shows little to no variations with surface temperature. At the 99.9th percentile, the ensemble mean value is around 90 mm d^{-1} with a 16% spread among the products. The sub ensemble is characterized by the same mean value and a 8% average spread over the regime. Similar behavior of the products is found at the 99th percentile, with a mean value of 49 mm d^{-1} and an ensemble (sub ensemble) spread of 13% (6%). Unlike the other products, the GPCC estimate expresses an increase of the two extreme percentile values with temperature within this regime.

3.2. The 'warm' regime (299 K<t2m <305 K)

This corresponds to ~17% of the total precipitation (figure 2). This regime is characterized by an overall decrease of the extreme precipitation with temperature attributed to the limited supply of moisture over these arid land regions (Westra *et al* 2014). For this regime, the more complex relationship between surface temperature, surface humidity and column humidity could also explain the negative scaling of the extreme precipitation (Roderick *et al* 2019). It is also important to note that this regime could be driven not only by thermodynamics but also by changes in the dynamics of the storms, with increasing surface temperature. While this negative scaling was explored with rain gauges data in the literature, it is well reproduced by the gridded products. The spread among the products of the ensemble is larger than for the previous regime especially at the warm end of the range for which very low sample is available (figure 2).

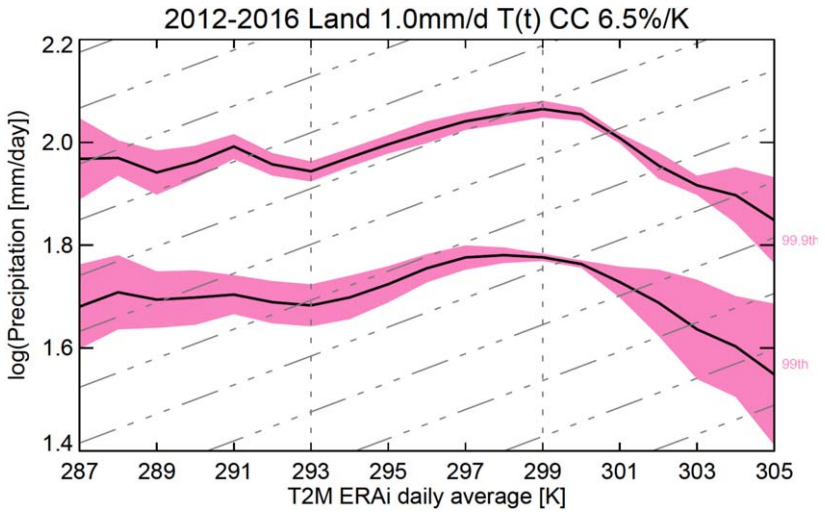

Figure 3. The value of the 99.9th and 99th percentiles of the 1° × 1° daily-accumulated precipitation over the tropical (30°s–30°n) land for the period 2012–2016 as a function of the 2 m daily temperature for the sub-set of the ensemble defined in the text (sENS). Shading is the standard deviation of the ensemble. The dashed dot gray lines correspond to the Clausius–Clapeyron 6.5%/K rate.

3.3. The 'Clausius–Clapeyron' regime (293 K ⩽ t2m ⩽299 K)

This regime accounts for ∼73% of the total precipitation (figure 2) and is characterized by an overall increase of the extreme precipitation with temperature across the regime. The spread among the products for the entire ensemble spans the 15%–25% range for all the three percentiles. The GPCC and PERSIANN products provides the highest and the lowest percentile values, respectively for the three cases contributing to the relative large spread of the whole ensemble. On the other hand, the sub ensemble again shows strong consistency with a small spread of 4%, 3% and 3% for the 99.9th, 99th and 90th percentiles. As discussed in the Introduction, theoretical considerations suggest that the rate of increase of the extreme precipitation in this regime is close to Clausius–Clapeyron that is 6%–7%/K. The slope of the regression (see Method in supplementary material) has been computed for each product for the 99.9th, 99th and 90th percentiles (table S2). The highest estimate is 6.2%/K for GSMArtg and the lowest 0.5%/K for GPCC. The entire ensemble mean slope is around ∼3%–4%/K for each percentiles values with a spread between 25% and 75%. When the sub ensemble is concerned, the 90th percentile scaling is 4.7% ± 17%. For the 99.9th and the 99th percentiles the spread among the products is reduced to ∼20% compared to the entire ensemble and the mean value of the slope is 5.2%/K. When the 299 K upper bound is changed to 300 or 298 K, the mean value of the slope becomes 4.7%/K or 5.6%/K showing little sensitivity to the precise location of the peak. Changing the lower bound to 292 K yields to a slightly lower 4.4%/K value also indicating the robustness of the 'Clausius–Clapeyron' regime for the sub ensemble of products.

4. Conclusions and discussion

Mean conditional precipitation (mean precipitation when precipitation is greater than 1 mm d^{-1}) is very consistent among the various products over the tropical land in agreement with previous analysis at a quasi-global scale (Herold *et al* 2017). The sub ensemble is significantly more robust than the entire ensemble. On the other hand, the full precipitation distribution, while looking alike within the ensemble members, can exhibit significant variance among the products, in particular at the high end of the precipitation spectrum. Sub setting the ensemble to a restricted selection of satellite products that includes microwave observations from a constellation of satellites partly mitigate this issue. In particular, up to 75 mm d^{-1}, the spread among the sub ensemble members is less than 10%. When sorted by surface temperature, the ensemble of gridded precipitation observations reveals a mean conditional precipitation distribution with a relatively small spread of the values well below 10% over a large span of the surface temperature regime. According to this metric, both the entire and the sub ensembles exhibit the same level of robustness.

The distribution of 'extreme' (∼110 mm d^{-1}) and 'moderate' (∼60 mm d^{-1}) extremes sorted by surface temperature regime again reveals a robust behavior among the products, in particular for the sub ensemble that is characterized by less than ∼10% relative spread in the highest percentile all through the considered surface temperature range from 287 to 305 K. Within that range, three distinct regimes are found in most of the product and in both the ensemble means that exhibit only a slight sensitivity to the percentile considered to delineate the temperature range of each regimes. The cold regime extends from 287 to 293 K, the increasing regime spans 293–299 K and the

decreasing regime is found over the warmest region from 299 to 305 K. Our results confirm previous elaboration about the decreasing regime after a peak temperature (Westra *et al* 2014). In our case, for the tropical land as a whole, a robust peak is observed around 299–300 K which is warmer than previous tropical rain gauges based analysis (Hardwick Jones *et al* 2010) although the difference between local observations and $1^\circ \times 1^\circ$ area averaged 2 m temperature analysis could explain this warm shift. Our analysis further indicates that a 'flat' regime characterizes the 'extreme' and 'moderate' extremes at the cold end of the temperature spectrum. From 287 to 293 K indeed the extremes show no dependence to surface temperature. Note also that for the 90th percentile, no such flat regime is observed; the range of value of this low percentile follow a bell shaped distribution. While the decreasing regime has been associated to limited humidity supply, the reasons for the flat regime are not clear. The 287–293 K regions could be related to orography or some seasonal features over tropical land areas that contribute to a steady value of the extreme, although high ($\sim$90 mm d^{-1} for the 'extreme' extremes case), over that range of surface temperature conditions. This new result warrants further investigation of these large daily rainfall accumulation extremes on the cold end of the spectrum.

In between these two regimes, across the 'increasing' regime, from 293 to 299 K, the scaling of the extreme precipitation to the surface temperature is investigated. For the entire ensemble, the 'extreme' extremes mean scaling is around 3%/K with a 75% spread within the ensemble. For the moderate extremes, the mean value is 3.4%/K respectively and the spread decrease to 45% consistent with the distribution spread variation with precipitation intensity (figure 1). When the sub ensemble is considered, a different perspective emerges with mean value $\sim$5%/K close to the tropical Clausius–Clapeyron for both the 'extreme' and the 'moderate' extremes. The robustness of the estimates is also better than for the entire ensemble with a relative spread of 19% and 20% for the 99.9th and 99th percentiles. This result are based on a renewed observational set of gridded products, depicted by recent versions of mainly satellite precipitation products and rules out any super-cc scaling for the $1^\circ \times 1^\circ$ daily extremes precipitation as well as the earlier proposed negative scaling (Utsumi *et al* 2011) or lack of scaling (Vittal *et al* 2016). This analysis further confirms the theoretical expectation (O'Gorman and Schneider 2009) for the tropical regions. As discussed in the Introduction, these results are valid for present climate conditions and should not be straight forwardly extrapolated for future climate conditions as the drivers for climate change in extreme may not be the same as the one acting in the present climate (Li *et al* 2019).

The three regimes identified here are linking the upper tail of the precipitation distribution to the surface temperature conditions. These are part of a larger scale co-variability of precipitation and temperature (Trenberth and Shea 2005) related to the large scale circulation. The analysis of the spatial and temporal distribution of these regimes and links to large-scale circulation shifts requires further studies. It is out of the scope of this Letter to explore these regimes further and it is deferred as a direction for future works.

Acknowledgments

This study benefited from the IPSL mesocenter ESPRI facility, which is supported by CNRS, UPMC, Labex L-IPSL, CNES and Ecole Polytechnique. The author acknowledges the CNES and CNRS support under the Megha-Tropiques program. The author thanks an anonymous reviewer and Dr Richard Allan for interesting comments that help improve this letter.

Data availability statement

The data that support the findings of this study are openly available. Precipitation datasets originates from the FROGS database DOI: https://doi.org/10.14768/06337394-73A9-407C-9997-0E380DAC5598. The ERA-interim surface temperature can be obtained from ECMWF.

ORCID iDs

Rémy Roca https://orcid.org/0000-0003-1843-0204

References

Ali H and Fowler H J 2018 Global observational evidence of strong linkage between dew point temperature and precipitation extremes *Geophys. Res. Lett.* **45** 320–30

Allan R and Liu C 2018 Evaluating large-scale variability and change in tropical rainfall and its extremes *Tropical Extremes: Natural Variability and Trends* ed V Vuruputur *et al* (Amsterdam: Elsevier) (https://doi.org/10.1016/B978-0-12-809248-4.0)

Bao J, Sherwood S C, Colin M and Dixit V 2017 The robust relationship between extreme precipitation and convective organization in idealized numerical modeling simulations *J. Adv. Model. Earth Syst.* **9** 2291–303

Barbero R, Westra S, Lenderink G and Fowler H J 2017 Temperature-extreme precipitation scaling: a two-way causality? *Int. J. Climatol.* **38** e1274–79

Beck H E *et al* 2017 Global-scale evaluation of 22 precipitation datasets using gauge observations and hydrological modeling *Hydrol. Earth Syst. Sci.* **21** 6201–17

Becker A, Finger P, Meyer-Christoffer A, Rudolf B, Schamm K, Schneider U and Ziese M 2013 A description of the global land-surface precipitation data products of the global precipitation climatology centre with sample applications including centennial (trend) analysis from 1901–present *Earth Syst. Sci. Data* **5** 71–99

Eiji E, Nobuyuki M and Taikan U 2012 Decreasing precipitation extremes at higher temperatures in tropical regions *Nat. Hazards* **64** 935–41

Fischer E M and Knutti R 2016 Observed heavy precipitation increase confirms theory and early models *Nat. Clim. Change* **6** 986–91

Gosset M, Viarre J, Quantin G and Alcoba M 2013 Evaluation of several rainfall products used for hydrological applications over West Africa using two high-resolution gauge networks *Q. J. R. Meteorol. Soc.* **139** 923–40

Gosset M, Viarre J, Quantin G, Alcoba M, Alcoba M, Roca R, Cloché S and Urbani G 2018 Evaluation of TAPEER daily estimates and other GPM era products against dense gauge networks in West Africa, analyzing ground reference uncertainty *Q. J. R. Meteorol. Soc.* (https://doi.org/10.1002/qj.3335)

Guilloteau C, Roca R and Gosset M 2016 A multiscale evaluation of the detection capabilities of high-resolution satellite precipitation products in West Africa *J. Hydrometeorol.* **17** 2041–59

Hardwick Jones R, Westra S and Sharma A 2010 Observed relationships between extreme sub-daily precipitation, surface temperature, and relative humidity *Geophys. Res. Lett.* **37** 1–5

Herold N, Behrangi A and Alexander L V 2017 Large uncertainties in observed daily precipitation extremes over land *J. Geophys. Res.* **122** 668–81

Joyce R J, Xie P, Janowiak J E, Arkin P A and Xie P 2004 CMORPH: a method that produces global precipitation estimates from passive microwave and infrared data at high spatial and temporal resolution *J. Hydrometeorol.* **5** 487–503

Kidd C, Kniveton D R, Todd M C, Bellerby T J, Becker A, Huffman G J, Muller C L, Joe P, Skofronick-Jackson G and Kirschbaum D B 2017 So, how much of the earth's surface is covered by rain gauges? *Bull. Am. Meteorol. Soc.* **98** 69–78

Levizzani V *et al* 2018 The activities of the international precipitation working group *Q. J. R. Meteorol. Soc.* **144** (Suppl. 1) 3–15

Li C, Zwiers F, Zhang X and Li G 2019 How much information is required to well constrain local estimates of future precipitation extremes? *Earth's Future* **7** 11–24

Liu C, Allan R P and Huffman G J 2012 Co-variation of temperature and precipitation in CMIP5 models and satellite observations *Geophys. Res. Lett.* **39** 1–8

Maggioni V, Meyers P C and Robinson M D 2016 A review of merged high-resolution satellite precipitation product accuracy during the tropical rainfall measuring mission (TRMM) era *J. Hydrometeorol.* **17** 1101–17

Muller C J, O'Gorman P A and Back L E 2011 Intensification of precipitation extremes with warming in a cloud-resolving model *J. Clim.* **24** 2784–800

O'Gorman P A 2012 Sensitivity of tropical precipitation extremes to climate change *Nat. Geosci.* **5** 697–700

O'Gorman P A 2015 Precipitation extremes under climate change *Curr. Clim. Change Rep.* **1** 49–59

O'Gorman P A and Schneider T 2009 The physical basis for increases in precipitation extremes in simulations of 21st-century climate change *Proc. Natl. Acad. Sci. USA* **106** 14773–7

Pfahl S, O'Gorman P A and Fishcer E M 2017 Understanding the regional pattern of projected future changes in extreme precipitation *Nat. Clim. Chang.* **7** 423–7

Ramanathan V 1981 The role of ocean-atmosphere interactions in the CO_2 climate problem *J. Atmos. Sci.* **38** 918–30

Roca R *et al* 2017 A simple model of the life cycle of mesoscale convective systems cloud shield in the Tropics *J. Clim.* **30** 4283–98

Roca R, Chambon P, Jobard I, Kirstetter P-E, Gosset M and Bergès J C 2010 Comparing satellite and surface rainfall products over West Africa at meteorologically relevant scales during the AMMA campaign using error estimates *J. Appl. Meteorol. Climatol.* **49** 715–31

Roderick T P, Wasko C and Sharma A 2019 Atmospheric moisture measurements explain increases in tropical rainfall extremes *Geophys. Res. Lett.* **46** 1375–82

Schär C *et al* 2016 Percentile indices for assessing changes in heavy precipitation events *Clim. Change* **137** 201–16

Stephens G L and Ellis T D 2008 Controls of global-mean precipitation increases in global warming GCM experiments *J. Clim.* **21** 6141–55

Singh M S and O'Gorman P A 2014 Influence of microphysics on the scaling of precipitation extremes with temperature *Geophys. Res. Lett.* **41** 6037–44

Taylor C M *et al* 2017 Frequency of extreme Sahelian storms tripled since 1982 in satellite observations *Nature* **544** 475–8

Trenberth K 2011 Changes in precipitation with climate change *Clim. Res.* **47** 123–38

Trenberth K E, Dai A, Rasmussen R M and Parsons D B 2003 The changing character of precipitation *Bull. Am. Meteorol. Soc.* **84** 1205–18

Trenberth K E and Shea D J 2005 Relationships between precipitation and surface temperature *Geophys. Res. Lett.* **32** 1–4

Utsumi N, Seto S, Kanae S, Maeda E E and Oki T 2011 Does higher surface temperature intensify extreme precipitation? *Geophys. Res. Lett.* **38** 1–5

Vittal H, Ghosh S, Karmakar S, Pathak A and Murtugudde R 2016 Lack of dependence of indian summer monsoon rainfall extremes on temperature: an observational evidence *Nat. Publ. Gr.* 1–12

Wang G, Wang D, Trenberth K E, Erfanian A, Yu M, Bosilovich M G and Parr D T 2017 The peak structure and future changes of the relationships between extreme precipitation and temperature *Nat. Clim. Chang.* **7** 268–74

Wasko C, Parinussa R M and Sharma A 2016 A quasi-global assessment of changes in remotely sensed rainfall extremes with temperature *Geophys. Res. Lett.* **43** 12659–68

Westra S and Sisson S A 2011 Detection of non-stationarity in precipitation extremes using a max-stable process model *J. Hydrol.* **406** 119–28

Westra S, Sisson S A, Alexander L V and Zwiers F W 2013 Global increasing trends in annual maximum daily precipitation *J. Clim.* **26** 3904–18

Westra S *et al* 2014 Future changes to the intensity and frequency of short-duration extreme rainfall *Rev. Geophys.* **52** 522–55